

Study on Damage Severity Assessment Methods for Asymmetrically Damaged Loitering Munitions

Mingxuan Zhang[1, 2], Yishan Zhang[3], Baigang Mi[1, 2, *], Yan Liu[1, 2]& Ruiqi Wang[1, 2]

[1] School of Aeronautics, Northwestern Polytechnical University, Xi'an 710072, China
[2] National Key Laboratory of Aircraft Configuration Design, Xi'an, 710072, China
[3] Chinese Flight Test Establishment, Xi'an, 710089, China
*Corresponding author. *E-mail address:* mibaigang@nwpu.edu.cn

Abstract

This paper investigates a loitering munition subjected to asymmetric damage. To address the mass loss, inertia variation, and aerodynamic force–moment coupling effects induced by asymmetric damage, a high-fidelity CFD-based approach is first employed to evaluate and identify the coupled static and dynamic derivatives of the damaged configuration. Compared with the intact configuration, the identified derivatives exhibit variations ranging from 7 to 17 times larger. Subsequently, damage-related parameters and longitudinal–lateral aerodynamic coupling corrections are incorporated into a conventional flight control model, leading to the establishment of a fully coupled flight control model capable of capturing the physical effects of asymmetric damage. PID-based control strategies are then applied to simulate the control response histories of the damaged munition. Finally, based on the actual mission profile of a loitering munition, quantitative damage-level criteria are proposed separately for the cruise phase and the terminal guidance attack phase. Damage-level assessments are conducted for the Harpy loitering munition subjected to asymmetric wing and vertical-tail damage. The results indicate that all investigated wing-damage cases are classified as Damage Level I, resulting in complete loss of control and mission capability. In contrast, the damage levels associated with asymmetric vertical-tail damage are primarily classified as Damage Levels II and III. Under these conditions, the munition retains the capability to perform cruise missions but largely loses its effectiveness in engaging designated targets.

Keywords: Asymmetric Damage; Dynamic Derivative Identification; Fully Coupled Flight Control Model; Damage-Level Criteria

1 Introduction

In recent years, loitering munition technology has advanced rapidly, with continuous improvements in flight performance, making loitering munitions an important strike platform on the modern battlefield. However, with the widespread deployment of various aerial interception weapons, the probability of loitering munitions sustaining damage due to airborne interception during mission execution has increased significantly[1],[4]~[7]. Damage to the wings, fuselage, and control surfaces degrades the aerodynamic performance of the munition. Moreover, asymmetric damage destroys the vehicle's geometric symmetry, resulting in a center-of-gravity shift and the generation of additional moments. These effects increase the trim burden on the flight control system, leading to deterioration in flight quality and even control system failure. In severe cases, the loitering munition may completely lose its strike capability. Therefore, assessing the effects of damage is essential for determining the remaining combat capability of damaged loitering munitions and is of great significance for battlefield decision-making and operational deployment[2]~[3].

Extensive research has been conducted on asymmetrically damaged aircraft. He et al. [8] employed a fuzzy neural network approach to compensate for uncertainties in flight control parameters caused by asymmetric aerodynamic characteristics. Du et al. [9] considered the mass offset induced by structural loss damage and developed an adaptive control system for damaged fixed-wing aircraft, enabling rapid attitude recovery under damage conditions. Dhiman [10] addressed failures and damage in aircraft fuselage and propulsion systems by combining approximate dynamic programming with neural network techniques, thereby improving the aircraft's dynamic characteristics. Miao et al. [11] introduced a damage factor into the longitudinal control equations to achieve adaptive longitudinal control of aircraft with damaged horizontal tails.

Overall, current studies on the dynamic characteristics of asymmetrically damaged loitering munitions have not incorporated damage-induced inertia variations and longitudinal–lateral aerodynamic coupling effects into the rigid-body state-space equations. As a result, existing control systems remain mathematically inconsistent with the actual physical phenomena associated with asymmetric damage, limiting their applicability to comprehensive damage-effect evaluation and the establishment of standardized damage-level criteria. To address these issues, a static and dynamic derivative identification method based on high-fidelity dynamic CFD data is first employed to determine the coupled dynamic derivatives induced by asymmetric damage. Subsequently, a fully coupled nonlinear dynamic model accounting for damage-induced effects is derived and reconstructed on the basis of conventional flight dynamics modeling. Finally, damage-level criteria for asymmetrically damaged loitering munitions are established according to the mission profile of the munition, providing a reference for the rapid assessment of post-damage combat capability.

2 Coupled Dynamic Derivative Calculation for Asymmetrically Damaged Loitering Munitions

2.1 Static and Dynamic Derivative Identification Based on High-Fidelity Dynamic CFD Data

In this study, the static and dynamic aerodynamic derivatives of asymmetrically damaged loitering munitions are identified using a high-fidelity dynamic CFD approach combined with the least-squares identification method. A forced-oscillation technique is employed, in which prescribed harmonic motion equations are imposed on the aircraft to induce small-amplitude pitching, rolling, and yawing motions about the center of gravity. The resulting time-history variations of aerodynamic force and moment coefficients with respect to the motion parameters are then obtained and analyzed. For the calculation of longitudinal aerodynamic data, a pitching oscillation motion is adopted, as expressed in Eq.(2.1), where α_m=1°.

$$\alpha = \alpha_m \sin(wt) \tag{2.1}$$

For the calculation of lateral–directional aerodynamic data, rolling and yawing oscillation motions are employed, as described by Eqs. (2.2) and (2.3), where ϕ_m=ψ_m=1°.

$$\phi = \phi_m \sin(wt) \tag{2.2}$$

$$\psi = \psi_m \sin(wt) \tag{2.3}$$

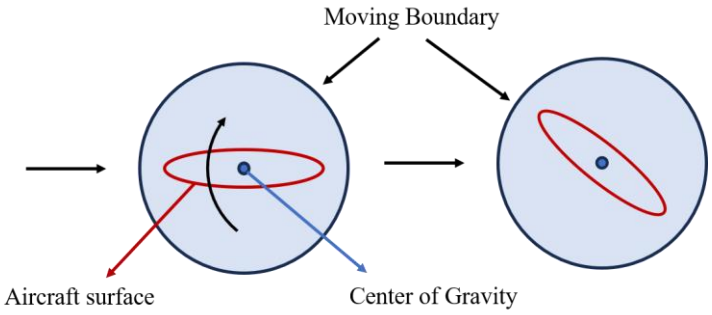


Fig 1 Forced-Oscillation Method

The reduced frequency k characterizes the oscillatory motion and is defined by Eq. (2.4). For longitudinal calculations, $\bar{c}$ denotes the mean aerodynamic chord, whereas for lateral–directional calculations, $\bar{c}$ represents the wingspan of the vehicle. Based on the specified reduced frequency, the oscillation periods corresponding to Eqs. (2.1)~(2.3) can be determined accordingly.

$$k = \frac{w\bar{c}}{2V} \tag{2.4}$$

Based on the time-domain data of unsteady aerodynamic forces and moments obtained from dynamic CFD simulations, an error function is established as given in Eq. (2.5). The static and dynamic aerodynamic derivatives are then identified using the least-squares method. Furthermore, the effects of different damage configurations on the identified derivatives are investigated and analyzed.

$$E(\theta) = \sum_{i=1}^{n} (y_i - f(x_i;\theta))^2 \tag{2.5}$$

2.2 Analysis of Coupled Dynamic Derivative Results for Asymmetrically Damaged Loitering Munitions

2.2.1 Description of Asymmetric Damage Configurations

In this study, a series of asymmetric damage configurations are designed for the Harpy loitering munition. The investigated damage cases include unilateral wing loss of 25%, 75%, and 100%, as well as unilateral vertical-tail loss of 25%, 75%, and 100%. Schematic illustrations of the corresponding damage configurations are shown in Fig 2.

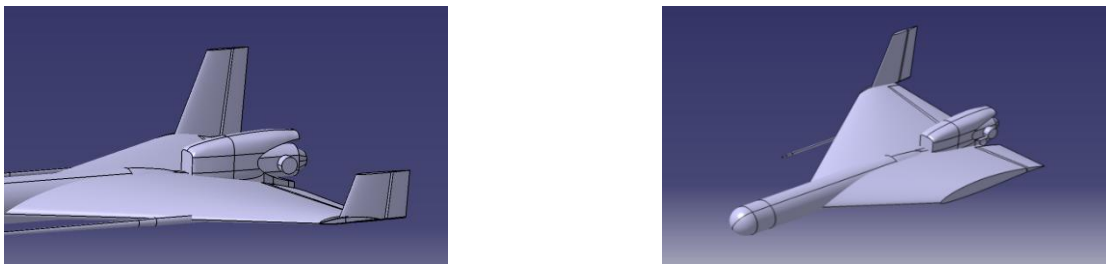


Fig 2 Asymmetric Damage Configurations

2.2.2 Analysis of Coupled Dynamic Derivatives

The identification results of the longitudinal–lateral directional coupled dynamic derivatives for the wing-loss damage configurations are presented in Fig 3~4. As can be observed from the figure, with the increasing extent of wing loss, Clα initially increases and then decreases. The maximum variation occurs for the 75% unilateral wing-loss configuration, with an increase of approximately 1700% compared with the intact configuration. The derivative Clq

exhibits a trend of increasing first, then decreasing, and finally increasing again, with the largest variation also occurring in the 75% unilateral wing-loss configuration, reaching approximately 700% relative to the intact configuration.In contrast, both Cnα and Cnq show a continuously decreasing trend as the wing-loss severity increases. The maximum variations are observed in the 100% unilateral wing-loss configuration, where the magnitudes of the changes reach approximately 1500% compared with those of the intact configuration.

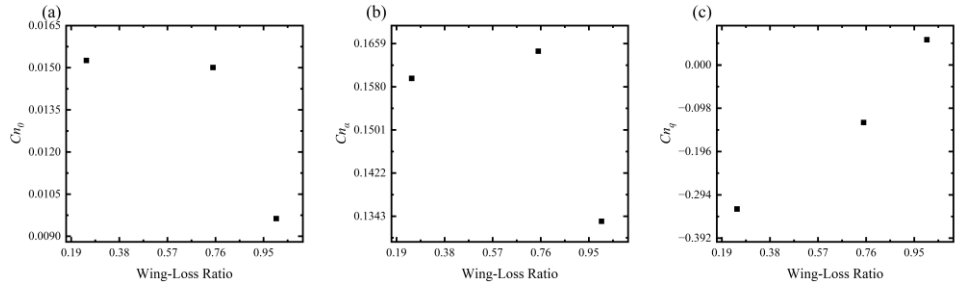


Fig 3 Comparison of the Identified Static and Dynamic Rolling-Moment Coupling Derivatives for Wing-Loss Damage Configurations

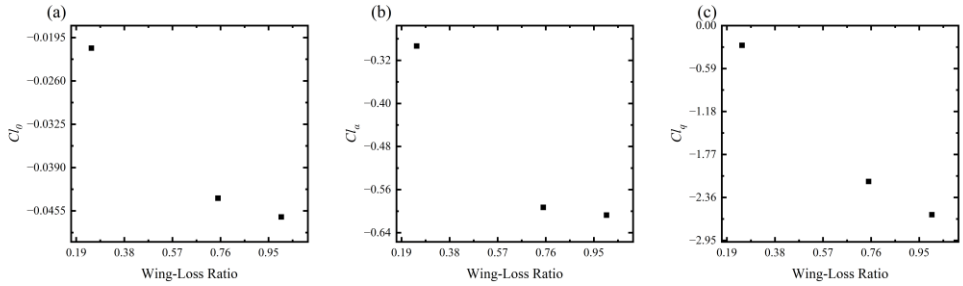


Fig 4 Comparison of the Identified Static and Dynamic Yawing-Moment Longitudinal Coupling Derivatives for Wing-Loss Damage Configurations

The identification results of the longitudinal–lateral directional coupled dynamic derivatives for the vertical-tail-loss damage configurations are shown in Fig 5~6. As can be observed from the figure, with the increasing extent of unilateral vertical-tail loss, Clα exhibits an increasing trend. The largest variation occurs in the 75% unilateral vertical-tail-loss configuration, reaching approximately 1200% relative to the intact configuration. The derivative Clq first decreases and then remains relatively stable as the damage severity increases. The maximum variation is also observed in the 75% unilateral vertical-tail-loss configuration, with a change of approximately 1600% compared with the intact configuration. In contrast, both Cnα and Cnq decrease progressively with increasing vertical-tail-loss severity. The largest variations occur in the 100% unilateral vertical-tail-loss configuration, where the changes reach approximately 1800% relative to the intact configuration.

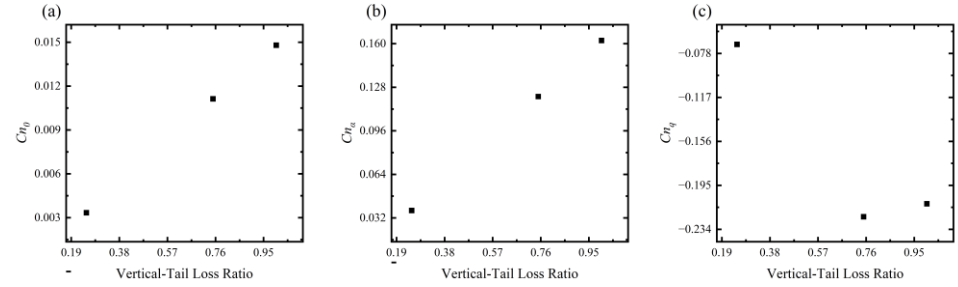


Fig 5 Comparison of the Identified Static and Dynamic Rolling-Moment Coupling Derivatives for Vertical-Tail-Loss Damage Configurations

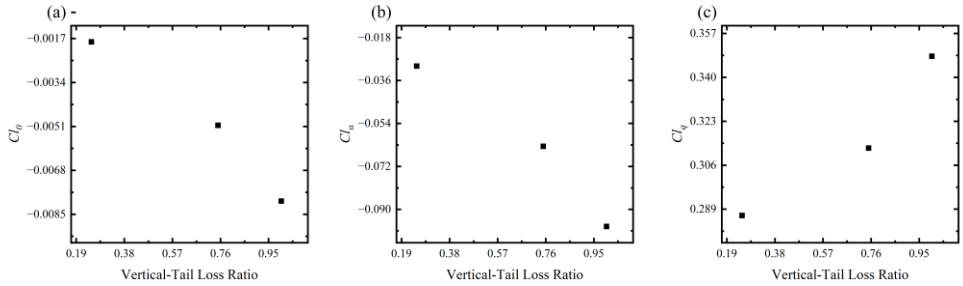


Fig 6 Comparison of the Identified Static and Dynamic Longitudinal-to-Yaw Coupling Derivatives

In summary, both wing-loss and vertical-tail-loss damage configurations have significant effects on the aircraft rigid-body state-space equations. In particular, substantial variations are observed in the coupled aerodynamic derivatives. These results indicate that severe asymmetric damage introduces pronounced longitudinal–lateral directional coupling effects, especially during longitudinal oscillatory motion. Consequently, for heavily damaged configurations, the coupling phenomena can no longer be neglected. Therefore, a fully coupled flight control model capable of capturing longitudinal–lateral directional interactions should be established in subsequent control system development and flight dynamics analysis.

3 Flight Control Model of a Loitering Munition Considering Asymmetric Damage

The conventional flight dynamics modeling framework is based on two fundamental decoupling assumptions.First, the longitudinal motion equations are decoupled from the lateral–directional motion equations. This decoupling relies on the existence of a longitudinal plane of symmetry, which leads to Ixy=Iyx=Iyz=Izy=0, After linearization of the moment equations and the introduction of the small-disturbance assumption, the corresponding mathematical relationships can be obtained, implying that the longitudinal aerodynamic moments depend only on the longitudinal motion variables. Second, the longitudinal aerodynamic moments are assumed to be decoupled from the lateral–directional aerodynamic moments. This assumption requires that the lateral–directional moments generated during longitudinal motion are negligible, thereby allowing the application of the conventional small-disturbance aerodynamic model. However, once asymmetric damage occurs, the geometric configuration and mass distribution symmetry of the loitering munition are destroyed. In addition, the imbalance of lift and drag forces between the two sides of the vehicle introduces significant coupling between the longitudinal and lateral–directional moments. Consequently, the two key assumptions underlying the conventional decoupled flight dynamics formulation become invalid. Therefore, the state-space equations for an asymmetrically damaged loitering munition must be re-derived by accounting for both the moment coupling induced by mass asymmetry and the aerodynamic moment coupling induced by asymmetric aerodynamic loads. To facilitate the derivation, the following assumptions are adopted in this study:(1) The instantaneous aerodynamic forces and moments depend only on the instantaneous flight state;(2) The aerodynamic forces and moments vary linearly with the motion variables, satisfying the small-disturbance aerodynamic model.

Based on these assumptions, the proposed flight control model can be represented by a system of eight first-order differential equations, which can be expressed as

$$\dot{x} = Ax + Bu \tag{3.1}$$

where x denotes the state vector of the state-space model, as defined in Eq. (3.2). Compared with the conventional flight control model, the system matrix A incorporates the effects of asymmetric damage, including mass loss, inertia variations, and longitudinal–lateral directional aerodynamic moment coupling. The vector u represents the control input vector, which is defined in Eq. (3.3):

$$x = [\Delta u \quad \alpha \quad q \quad \Delta\theta \quad \beta \quad \phi \quad p \quad r]^T \tag{3.2}$$

$$u = [\delta_e \quad \delta_a \quad \delta_r] \tag{3.3}$$

In contrast to the conventional state-space formulation of a loitering munition, in which the longitudinal and lateral–directional dynamics are treated separately, the state-space equations of an asymmetrically damaged vehicle exhibit strong aerodynamic moment coupling due to the asymmetric products of inertia induced by mass loss and the longitudinal–lateral directional coupled aerodynamic characteristics. Consequently, the damaged flight vehicle must be described using a fully coupled dynamic model. In the proposed formulation, A denotes the system matrix, B denotes the control effectiveness matrix, which can be expressed as fallow Eqs.

$$A = \begin{bmatrix}
(C_{xu}+\xi_1 C_{zu})/m_1 & (C_{x\alpha}+\xi_1 C_{z\alpha})/m_1 & (C_{xq}+\xi_1(m_1+C_{zq}c_1))/m_1 & (C_{x\theta}+\xi_1 C_{z\theta})/m_1 & 0 & 0 & 0 & 0 \\
C_{zu}/m_1 & C_{z\alpha}/m_1 & (m_1+C_{zq}c_1)/m_1 & C_{z0}/m_1 & 0 & 0 & 0 & 0 \\
I_{M1}a_{21}/I & (I_{M1}a_{22}+I_{L1}C_{l\alpha}+I_{N1}C_{n\alpha})/I & (I_{M1}a_{23}+b_1(I_{L1}C_{lq}+I_{N1}C_{nq}))/I & I_{M1}a_{24}/I & (I_{L1}a_{31}+I_{N1}a_{41})/I & (I_{L1}a_{32}+I_{N1}a_{42})/I & (I_{L1}a_{33}+I_{N1}a_{43})/I & (I_{L1}a_{34}+I_{N1}a_{44})/I \\
0 & 0 & 1 & 0 & 0 & 0 & 0 & 0 \\
0 & 0 & 0 & 0 & C_{y\beta}/m_1 & C_{y\phi}/m_1 & (C_{yp}b_1)/m_1 & -(m_1-C_{yr}b_1)/m_1 \\
0 & 0 & 1 & 0 & 0 & 0 & 1 & 0 \\
(I_{M2}a_{21})/I & (I_{M2}a_{22}+I_{L2}C_{l\alpha}+I_{N2}C_{n\alpha})/I & (I_{M2}a_{23}+b_1(I_{L2}C_{lq}+I_{N2}C_{nq}))/I & (I_{M2}a_{24})/I & (I_{L2}a_{31}+I_{N2}a_{41})/I & (I_{L2}a_{32}+I_{N2}a_{42})/I & (I_{L2}a_{33}+I_{N2}a_{43})/I & (I_{L2}a_{34}+I_{N2}a_{44})/I \\
(I_{M3}a_{21})/I & (I_{M3}a_{22}+I_{L3}C_{l\alpha}+I_{N3}C_{n\alpha})/I & (I_{M3}a_{23}+b_1(I_{L3}C_{lq}+I_{N3}C_{nq}))/I & (I_{M3}a_{24})/I & (I_{L3}a_{31}+I_{N3}a_{41})/I & (I_{L3}a_{32}+I_{N3}a_{42})/I & (I_{L3}a_{33}+I_{N3}a_{43})/I & (I_{L3}a_{34}+I_{N3}a_{44})/I
\end{bmatrix} \tag{3.4}$$

$$B = \begin{bmatrix}
(C_{x\delta_e}+\xi_1 C_{z\delta_e})/m_1 & 0 & 0 \\
C_{z\delta_e}/m_1 & 0 & 0 \\
(I_{M1}a_{25})/I & (I_{L1}a_{35}+I_{N1}a_{45})/I & (I_{L1}a_{36}+I_{N1}a_{46})/I \\
0 & 0 & 0 \\
0 & C_{y\delta_a}/m_1 & C_{y\delta_r}/m_1 \\
0 & 0 & 0 \\
(I_{M2}a_{25})/I & (I_{L2}a_{35}+I_{N2}a_{45})/I & (I_{L2}a_{36}+I_{N2}a_{46})/I \\
(I_{M3}a_{25})/I & (I_{L3}a_{35}+I_{N3}a_{45})/I & (I_{L3}a_{36}+I_{N3}a_{46})/I
\end{bmatrix} \tag{3.5}$$

4 Development of Damage-Level Criteria for Asymmetrically Damaged Loitering Munitions

4.1 Operational Mission Profile of a Loitering Munition

During combat operations, the flight mission of a loitering munition can generally be divided into three phases: the launch and deployment phase, the loitering phase, and the terminal dive attack phase. During the launch phase, the munition is accelerated to its operational flight condition under relatively high overloads. At this stage, the onboard electronic systems remain powered off and the flight control system is inactive. During the deployment phase, the wings and control surfaces are unfolded, and the vehicle is stabilized and transitioned into the loitering phase. The loitering phase typically employs trajectory-tracking guidance to navigate toward the target area. Upon arrival, the munition performs target reconnaissance and surveillance, and prepares for engagement once the target has been identified and locked. The terminal dive attack phase generally adopts terminal guidance techniques to achieve precise target engagement and destruction. During the launch and deployment phases, the loitering munition is typically outside the effective engagement range of battlefield high-energy weapon systems. Consequently, the probability of sustaining combat damage during these phases is relatively low.

Therefore, this study focuses on the development of damage-level criteria for the loitering phase and the terminal dive attack phase, where the munition is more likely to be exposed to high-energy weapon threats.

4.2 Damage-Level Criteria for the Loitering Phase

During the loitering phase, the primary mission of a loitering munition is to search for and locate targets. The vehicle typically performs a loitering flight pattern and maintains a relatively steady flight condition for an extended period. Therefore, when subjected to an attack from a high-energy weapon during this phase, the flight control system detects the resulting attitude perturbations and attempts to restore the munition to its nominal loitering condition. Specifically, the control system regulates the angle of attack, pitch angle, yaw angle, and roll angle to recover the original flight attitude and maintain mission execution.

However, different impact locations and damage severities produced by high-energy weapon attacks result in varying levels of structural damage, which in turn affect the controllability of the damaged munition. Consequently, the flight control system may exhibit different response characteristics, including rapid convergence, slow convergence, or even divergence. Therefore, for the loitering phase, the effectiveness of attitude stabilization following damage is adopted as the primary criterion for damage-level assessment. A damage-level criterion based on attitude recovery time is proposed, which can also be reflected in the corresponding trajectory deviation after damage.

Specifically, the control process following damage is analyzed by evaluating the period from the instant of impact to the recovery of the original flight condition under flight control intervention. The convergence characteristics of the flight-path angle are used as the principal evaluation metric. According to the flight-path-angle convergence-time criteria listed in Table 1, the capability of the damaged loitering munition to continue its mission can be comprehensively assessed. If the trajectory deviation exceeds a prescribed threshold or exhibits a clear divergence trend, the damage state is classified as uncontrollable, indicating a severe level of damage.

The damage levels are defined according to the following criteria. Let T0 denote the attitude convergence time of the intact configuration. The threshold values are defined as T1= 2T0，T2= 3T0. The corresponding damage-level classification is given as follows.

Table 1 Damage-Level Classification Criteria for the Loitering Phase

Damage Level	Assessment Parameter	Definition	Description
Level I	Flight-path-angle response, which directly reflects flight trajectory deviations	Flight-path-angle convergence time≥T_2	After sustaining damage, the loitering munition cannot be restored to its nominal flight condition within T_2, or requires more than T_2 to achieve recovery. Under such conditions, significant trajectory deviations occur, and the munition is unable to continue its mission.
Level II		T_2≥Flight-path-angle convergence time≥T_1	After sustaining damage, the flight-path angle cannot be restored to its nominal value within T_1. However, through control-surface deflections and propulsion-assisted stabilization, the flight control system successfully recovers the original flight condition within T_2.
Level III		Flight-path-angle convergence time≤T_1	After sustaining damage, the munition remains controllable. The flight control system stabilizes the

	vehicle through control-surface deflections and propulsion compensation, and the flight-path angle is restored to its nominal value within T_1.

4.3 Damage-Level Criteria for the Terminal Dive Attack Phase

During the terminal guidance attack phase, the primary mission of the loitering munition is to achieve precise target engagement. Once a target is detected, the munition transitions from the loitering phase to the attack phase. The propulsion system is commanded to operate at maximum thrust to increase flight speed and maneuverability, while the guidance and control system receives seeker guidance signals and directs the vehicle toward the target to accomplish a precision strike.When the munition sustains damage from a high-energy weapon during this phase, the flight control system must perform two successive control tasks:(1) Recover the damaged munition to its nominal terminal attack attitude;(2) After the original attack attitude has been recovered, account for the position deviation caused by the damage, generate an updated attack trajectory, and command the munition to track the newly determined terminal attack attitude in order to complete the engagement mission.Therefore, during the first control stage, a damage-level criterion based on attitude convergence time is established, following the same principle adopted for the loitering phase. The assessment focuses on the flight control system's ability to restore the damaged munition to its nominal attack attitude, and the corresponding performance can be reflected by the resulting trajectory deviation. However, since the munition operates at maximum thrust during the terminal attack phase, angle-of-attack control is no longer a primary concern. Consequently, only the pitch, roll, and yaw control channels are considered in the assessment.During the second control stage, the munition has entered the final engagement phase, and the secondary attitude adjustment directly affects terminal guidance accuracy. Therefore, the damage-level assessment in this stage is based on terminal guidance accuracy, which serves as the primary evaluation metric.It should be noted that the damage level for the terminal guidance attack phase is determined through a two-step assessment procedure. First, the damage level corresponding to the attitude-recovery stage is evaluated. Second, the damage level associated with terminal guidance accuracy is determined. The higher of the two damage levels is taken as the final damage classification for the corresponding damage configuration during the terminal guidance attack phase.

For the first control stage, the damage levels are classified according to the following criteria. Let T0 denote the attitude convergence time of the intact configuration. Since the duration of the terminal guidance attack phase is significantly shorter than that of the loitering phase, the threshold values are redefined as T1= 2T0，T2= 3T0.The corresponding damage-level classification is defined as follows.

Table 2 Damage-Level Classification Criteria for Control Stage I of the Terminal Guidance Attack Phase

Damage Level	Assessment Parameter	Definition	Description
Level I	Flight-path-angle response, which directly reflects trajectory deviations	Flight-path-angle convergence time≥T_2	After sustaining damage, the loitering munition cannot be restored to its nominal attack condition within T_2, or requires more than T_2 to achieve recovery. Significant trajectory deviations occur, rendering the munition incapable of completing its attack mission.
Level II		T_2≥Flight-path-angle convergence	After sustaining damage, the flight-path angle cannot be restored to its nominal value within T_1. However, through control-surface deflections

		time≥T_1	and propulsion-assisted stabilization, the flight control system successfully recovers the nominal attack condition within T_2.
Level III		Flight-path-angle convergence time≤T_1	After sustaining damage, the munition remains controllable. The flight control system stabilizes the vehicle through control-surface deflections and propulsion compensation, and the flight-path angle is restored to its nominal value within T_1.

For the second control stage, the damage levels are classified according to the terminal guidance accuracy of the damaged loitering munition. Let R0 denote the effective strike radius of the intact loitering munition, within which effective target damage can be achieved. The threshold values are defined as R1= R0，R2= 5R0. The corresponding damage-level classification criteria are defined as follows.

Table 3 Damage-Level Classification Criteria for Control Stage II of the Terminal Guidance Attack Phase

Damage Level	Assessment Parameter	Definition	Description
Level I	Distance between the impact point of the damaged loitering munition and that of the intact configuration	Impact-point deviation≥R_2	After sustaining damage during Control Stage I, the loitering munition continues the engagement mission under the guidance and propulsion systems. However, the final impact point deviates from the target location by more than (R_2), exceeding both the effective strike radius and the severe-damage radius of the warhead. Consequently, effective damage against either equipment targets or personnel targets cannot be achieved, and the munition is considered combat ineffective.
Level II		R_2≥Impact-point deviation≥R_1	After sustaining damage during Control Stage I, the munition continues its attack mission. The final impact-point deviation exceeds the effective strike radius against equipment targets, resulting in the loss of effective equipment-engagement capability. However, the impact point remains within the severe-damage radius, allowing effective engagement of personnel targets.
Level III		Impact-point deviation≤R_1	After sustaining damage during Control Stage I, the munition continues the attack mission under guidance and propulsion control. The final impact-point deviation remains within the effective strike radius, and the munition retains its capability to inflict effective damage on the intended target.

5 Damage-Level Assessment of Asymmetrically Damaged Loitering Munitions

5.1 Damage-Level Assessment for the Loitering Phase

Figure X presents the control-channel response histories of different damage configurations obtained using the PID control system. Among the investigated damage cases, wing-loss damage exhibits the most significant impact on flight performance. For all wing-loss configurations, the loitering munition experiences substantial degradation in controllability during the loitering phase and is unable to recover its nominal loitering condition after sustaining damage. In particular, the 75% and 100% unilateral wing-loss configurations result in a complete loss of control authority, leading to flight control system failure. In contrast, the loitering munition subjected to vertical-tail-loss damage retains a relatively high level of controllability because its primary lifting surfaces remain largely intact. Furthermore, the mission performance during the loitering phase is less sensitive to heading deviations. As a result, the damaged munition is still capable of maintaining stable loitering flight and continuing the loitering mission after sustaining vertical-tail damage.

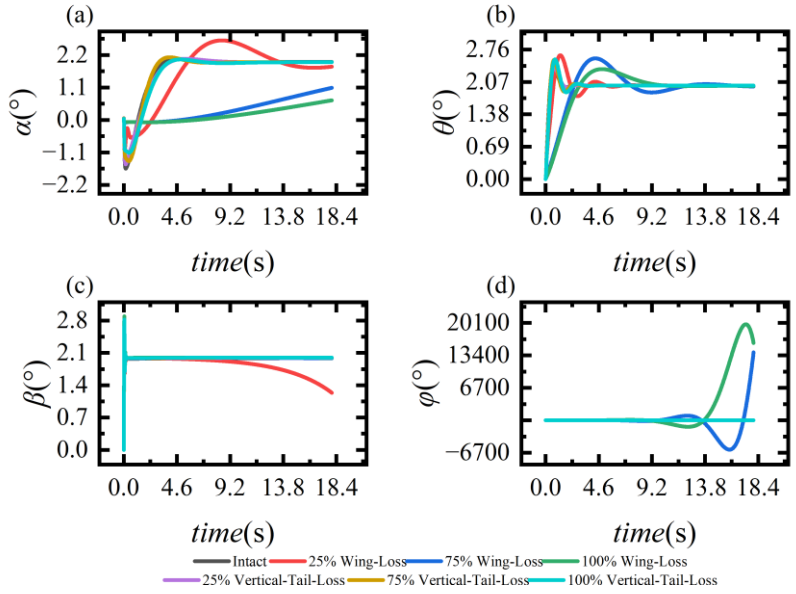


Fig 7 Response Histories of Each Control Channel

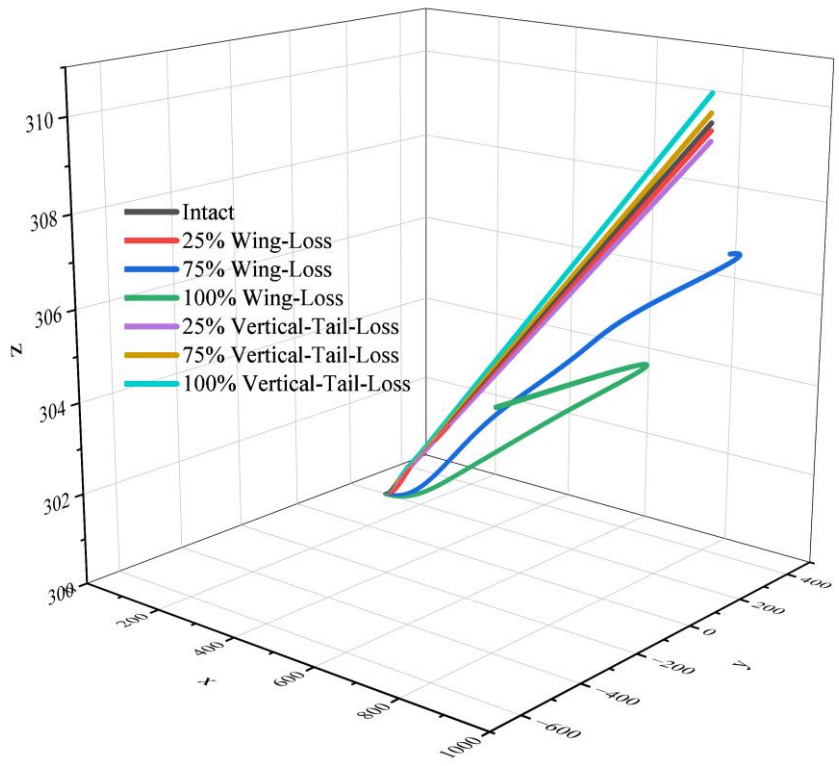


Fig 8 Flight Trajectories of Different Damage Configurations

According to the damage-level assessment results for the loitering phase, all wing-loss damage configurations are classified as Level I damage. Moreover, significant trajectory deviations are observed for the 75% and 100% unilateral wing-loss configurations, indicating a severe loss of flight controllability. In these cases, the loitering munition is unable to maintain its nominal flight condition and consequently loses its operational effectiveness. By contrast, the vertical-tail-loss damage configurations are classified as Level III damage. No significant trajectory deviation is observed during the loitering phase, indicating that the munition retains the capability to maintain stable flight and continue its loitering mission. These results suggest that effective interception of loitering munitions can still be achieved by deliberately targeting critical structural locations and damage severities that are prone to inducing loss-of-control behavior. Such targeted engagements can significantly enhance the defensive effectiveness of high-energy weapon systems against loitering munitions.

Table 4 Damage-Level Assessment of Damaged Harpy Configurations

Configuration	Control Channel 1	Control Channel 2	Control Channel 3	Control Channel 4	Overall Damage Level
Intact	Level III	Level III	Level III	Level III	Level III
25% Unilateral Wing-Loss	Level I	Level I	Level III	Level I	Level I
75% Unilateral Wing-Loss	Level I	Level I	Level III	Level I	Level I
100% Unilateral Wing-Loss	Level I	Level I	Level III	Level I	Level I

25% Unilateral Vertical-Tail-Loss	Level III	Level III	Level III	Level III	Level III
75% Unilateral Vertical-Tail-Loss	Level III	Level III	Level III	Level III	Level III
100% Unilateral Vertical-Tail-Loss	Level III	Level III	Level III	Level III	Level III

5.2 Damage-Level Assessment for the Terminal Guidance Attack Phase

During Control Stage I, the angle-of-attack control is not considered due to the maximum-thrust condition in the terminal guidance attack phase. The response histories of the pitch angle, roll angle, and sideslip angle control channels are shown in Fig 9. As can be observed from the figure, the 75% and 100% unilateral wing-loss configurations exhibit control instability during Control Stage I, corresponding to Level I damage. This behavior is reflected in the trajectory as significant deviations from the nominal flight path. In contrast, the vertical-tail-loss configurations do not show obvious loss of control during Control Stage I. Only a slower convergence is observed in the pitch-angle control channel. These cases are therefore classified as Level II damage, while the overall flight condition remains controllable.

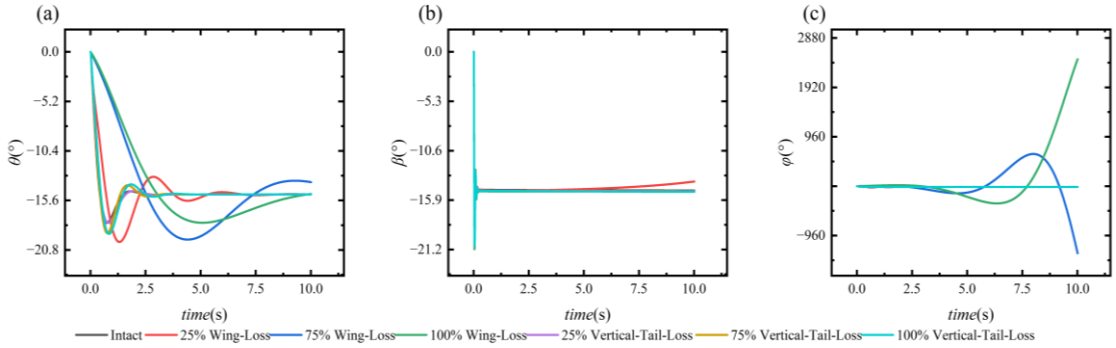


Fig 9 Response Histories of Each Control Channel

Table 5 Damage-Level Assessment of Damaged Harpy Configuration

Configuration	Control Channel 2	Control Channel 2	Control Channel 2	Control Channel 2
Intact	Level III	Level III	Level III	Level III
25% Unilateral Wing-Loss	Level I	Level III	Level I	Level I
75% Unilateral Wing-Loss	Level I	Level III	Level I	Level I
100% Unilateral Wing-Loss	Level I	Level III	Level I	Level I
25% Unilateral Vertical-Tail-Loss	Level III	Level III	Level III	Level III
75% Unilateral Vertical-Tail-Loss	Level III	Level III	Level III	Level III
100% Unilateral Vertical-Tail-Loss	Level II	Level III	Level III	Level II

During Control Stage II, the damage assessment based on the impact-point distribution of the loitering munition indicates that all wing-loss configurations are classified as Level I damage, corresponding to a complete loss of controllability. In these cases, the munition is unable to achieve effective engagement against equipment targets. For

vertical-tail-loss and wing-perforation damage configurations, the damage levels are mainly concentrated in Level II and Level III. Although partial controllability is retained, the impact points are predominantly located near the boundary of the effective damage radius of equipment targets. As a result, the capability to inflict effective damage on equipment is largely degraded. These findings demonstrate that interception by high-energy weapon systems remains effective against such damage conditions.

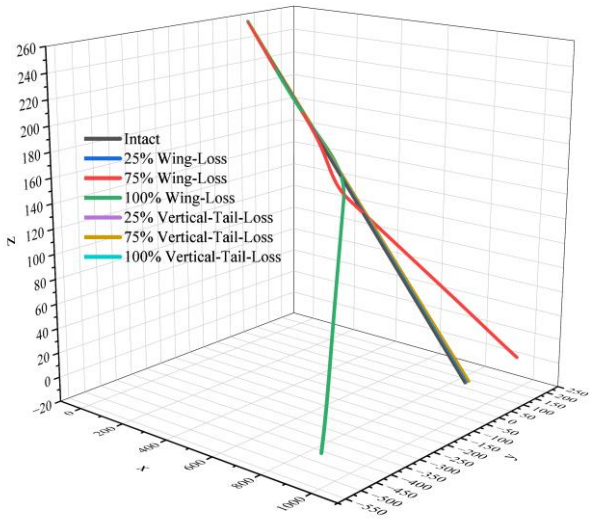


Fig 10 Flight Trajectories of Damage Configurations after Control Stages I and II in the Terminal Guidance Attack Phase

Table 6 Overall Damage Level Assessment of Damaged Harpy Configuration

Configuration	Overall Damage Level for Control Stage II	Overall Damage Level for Control Stage I	Overall Damage Level for Control
Intact	Level III	Level III	Level III
25% Unilateral Wing-Loss	Level II	Level I	Level I
75% Unilateral Wing-Loss	Level I	Level I	Level I
100% Unilateral Wing-Loss	Level I	Level I	Level I
25% Unilateral Vertical-Tail-Loss	Level III	Level III	Level III
75% Unilateral Vertical-Tail-Loss	Level II	Level III	Level II
100% Unilateral Vertical-Tail-Loss	Level III	Level II	Level II

6 Conclusion

This study considers the geometric and mass asymmetry as well as the coupled moment effects induced by asymmetric damage. First, a coupled set of dynamic derivatives resulting from asymmetric damage is identified based on high-fidelity unsteady CFD data using a static and dynamic derivative identification method. Subsequently, a fully coupled nonlinear flight dynamics model incorporating asymmetric damage effects is derived and reconstructed from

the conventional flight mechanics formulation. Finally, a damage-level assessment criterion for the flight performance degradation of loitering munitions under mission scenarios is established. The proposed method is applied to a certain type of loitering munition with asymmetric wing-loss and vertical-tail-loss damage configurations. The results indicate that the wing-loss damage cases are classified as Level I damage in both the loitering phase and the terminal guidance attack phase, corresponding to a complete loss of controllability and combat effectiveness after damage. In contrast, the vertical-tail-loss damage cases are mainly classified as Level II and Level III in both phases. Although the munition retains the capability to perform the loitering mission, its ability to effectively engage equipment targets is largely degraded.

Funding

Natural Science Foundation of Chongqing(GrantNo.CSTB2023NSCQ-MSX0042).

Copyright Statement

The authors confirm that they, and/or their company or organization, hold copyright on all of the original material included in this paper. The authors also confirm that they have obtained permission, from the copyright holder of any third party material included in this paper, to publish it as part of their paper. The authors confirm that they give permission, or have obtained permission from the copyright holder of this paper, for the publication and distribution of this paper as part of the ICAS proceedings or as individual off-prints from the proceedings.

References

[1] Duan Ruxuan, Huang Zhe. Review of patent technologies for UAV interception[J]. China Military–Civilian Conversion, 2024(17): 28–29.

[2] Konokman, Hüseyin Emrah, Kayran A , Kaya M .Aircraft vulnerability assessment against fragmentation warhead[J].Aerospace Science & Technology, 2017, 67:215-227.

[3] Mou H , Xie J , Feng Z ,et al.Review on the crashworthiness design and evaluation of fuselage structure for occupant survivability[J].Progress in Aerospace Sciences, 2024, 148:101001.1-18.

[4] Zhou Deyuan, Li Jie, Li Ligong. Study on damage effectiveness of anti-UAV laser weapons[J]. Laser & Infrared, 2025, 55(04): 546–553.

[5] WANG Zhe,XU Ling-fei,GU Chun-feng. Simulation of damage effect of laser weapon system against composite Unmanned Aerial Vehicle[J]. Air Space Defense,2018,1(1):63-68.

[6] XU Ming-xin,LIN Bing-xuan,CHEN Zhi-gang,et al. Analysis on technical approaches of medium/small Unmanned Aerial Vehicle against laser weapon[J]. Modern Defense Technology,2020,48(5):10-15.

[7] LI Chao-long,LI Ming-hui,CHEN Yu-hua. The application of laser weapon in the army's whole area operation[J].Laser Infrared,2020,50(5):515-520.

[8] He H, Meng X, Fan X. Neural-network-based dynamic flight envelop protection within integrated aircraft control system. Journal of Guidance, Control, and Dynamics. 2023 Jun;46(6):1083-94

[9] Du, Z., Lyu, Y., Zhai, X., Shi, J., & Qu, X. (2025). Fault-Tolerant Control for Fixed-Wing Aircraft with Asymmetric Damage: Model, Method, and Experiment. Journal of Guidance, Control, and Dynamics, 2021,48(5), 1004-1024

[10] Dhiman G, Tiumentsev YV, Tskhai RA. Combined Use of Dynamic Inversion and Reinforcement Learning for Motion Control of an Supersonic Transport Aircraft. Optical Memory and Neural Networks. 2024 Dec;33(Suppl 3):S399-413.

[11] Miao Y, Wang X, Miao Y, et al. Dynamics and adaptive fault-tolerant flight control under structure damage of horizontal stabilizer[J]. Aerospace Science and Technology, 2020, 106: 106135.